

# HiMTok: Learning Hierarchical Mask Tokens for Image Segmentation with Large Multimodal Model

Tao Wang<sup>\*1</sup>, Changxu Cheng<sup>\*†1</sup>, Lingfeng Wang<sup>\*2</sup>, Senda Chen<sup>\*3</sup>, Wuyue Zhao<sup>1</sup>

<sup>1</sup>Uni-Ubi <sup>2</sup>Zhejiang University <sup>3</sup>Tongji University

{wangtaomaruvel, ccx0127, sendachen586}@gmail.com, yayafengzi@zju.edu.cn, zhaohongyi@uni-ubi.com

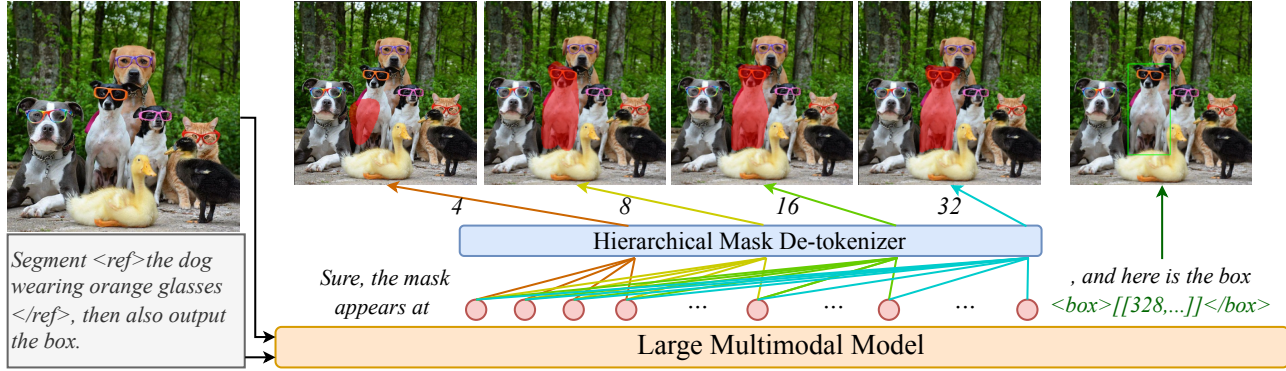


Figure 1. The Large Multimodal Model integrated with HiMTok can progressively generate masks from coarse to fine, enhancing visual grounding capabilities. In the figure, mask tokens of varying lengths (4, 8, 16, and 32) represent different levels of granularity.

## Abstract

The remarkable performance of large multimodal models (LMMs) has attracted significant interest from the image segmentation community. To align with the next-token-prediction paradigm, current LMM-driven segmentation methods either use object boundary points to represent masks or introduce special segmentation tokens, whose hidden states are decoded by a segmentation model requiring the original image as input. However, these approaches often suffer from inadequate mask representation and complex architectures, limiting the potential of LMMs. In this work, we propose the **Hierarchical Mask Tokenizer (HiMTok)**, which represents segmentation masks with up to 32 tokens and eliminates the need for the original image during mask de-tokenization. HiMTok allows for compact and coarse-to-fine mask representations, aligning well with the LLM next-token-prediction paradigm and facilitating the direct acquisition of segmentation capabilities. We develop a 3-stage training recipe for progressive learning of segmentation and visual capabilities, featuring a hierarchical mask loss for effective coarse-to-fine learning. Additionally, we enable bidirectional information flow, allowing conversion between bounding boxes and mask tokens to fully

leverage multi-task training potential. Extensive experiments demonstrate that our method achieves state-of-the-art performance across various segmentation tasks, while also enhancing visual grounding and maintaining overall visual understanding. The codes are available at <https://github.com/yayafengzi/LMM-HiMTok>.

## 1. Introduction

With the rapid development of large multimodal models (LMMs), visual capabilities are advancing toward more generalized forms [1, 13, 16, 35, 36, 62, 69]. Image segmentation, a fundamental task in computer vision, has recently improved in terms of generalization and instruction-following ability through integration with LMMs [27, 49, 76, 78]. Since large language models (LLMs) were originally designed to generate only text tokens, developing an appropriate representation for image segmentation is both critical and challenging.

There are several paradigms for LLM-based image segmentation. Some works represent a segmentation mask as a sequence of boundary points, which can be learned by a sequence-to-sequence framework [7, 44, 58, 83, 84], as shown in Fig. 2 (a). However, using a **limited number of polygon vertices** can impede accuracy, particularly in representing masks of complex shapes or multi-

<sup>\*</sup>Equal contributions.

<sup>†</sup>Corresponding author.

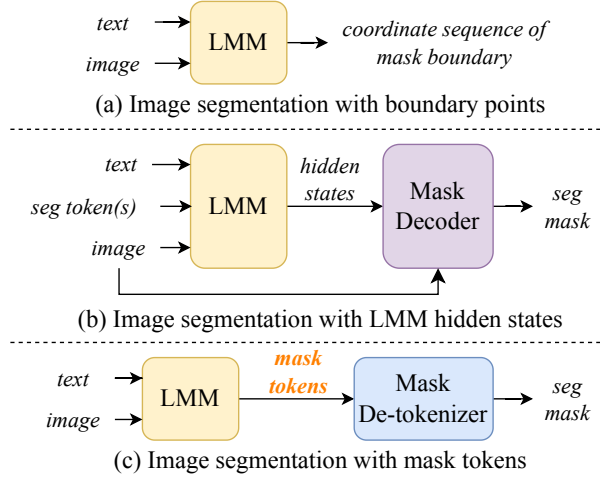


Figure 2. The three paradigms for LLM-based image segmentation. (a) Masks are represented as point sequences of boundaries. LMM output the coordinates directly. (b) LMM acts as a soft prompt generator for the image-conditioned mask decoder. (c) Ours. The LMM generates discrete mask tokens in the same manner as it generates text, and the mask de-tokenizer then converts these tokens into masks. This straightforward yet effective approach is enabled by our HiMTok.

ple regions [44, 84]. Some other LMM-based segmentation methods [2, 27, 47, 49, 61, 64, 76, 78] exploit LLMs to output object hidden states, which are subsequently passed to an additional image-conditioned mask decoder, as shown in Fig. 2 (b). Such hidden states usually correspond to some special learnable tokens (e.g., `<SEG>` [27]) to adapt to the next-token-prediction paradigm. However, there are three limitations to this paradigm. First, due to **the reliance on powerful image segmentation models**, large language models (LLMs) have insufficient learning of precise spatial localization in images. Second, there is **an inconsistency in mask representation between LLM input and output**. Special tokens serve solely as identifiers and are used as LLM input, resulting in the loss of crucial information from the corresponding hidden states in autoregressive modeling. If users provide mask prompts, they need to extract input prompt features through RoI pooling or cross-attention with visual features [76, 78]. Third, **the overall architecture is complex and heavy**. The mask decoder is typically designed on previous segmentation models and requires the original image to be used again, such as SAM [26] and Mask2Former [14], with some even requiring an additional vision encoder. Overall, these limitations restrict LLMs from achieving their full potential in image segmentation.

Some early methods view image segmentation as an image generation task [3, 39], offering a possible way to address the aforementioned limitations. By quantizing a mask image into 2D discrete tokens, it is promising to integrate the segmentation mask into LLM input and output sequence

consistently. Although the color space of masks is relatively simple, it is non-trivial and essential that the output mask *not only captures the object position but also maintains fine-grained shape details*, e.g., object boundary. VQ-GAN [17] is often used for image quantization that results in a 2D token matrix. Nonetheless, **2D token representation is very redundant** for a binarized mask image. Besides, **autoregressive patch-wise 2D token prediction has not yet shown very competitive performance** in image generation [54]. These facts pose a challenge for effective mask representation in LMM-based image segmentation.

In this work, we propose **HiMTok**, an effective **Hierarchical Mask Tokenizer** that can represent a mask image using up to 32 hierarchical tokens. Inspired by TiTok [74], images can be expressed as highly compact 1D sequences. Based on this concept, we introduce a hierarchical mask tokenizer that uses hierarchical mask loss and a causal attention mechanism to **represent mask images from coarse to fine, which can be learned from abundant and easily accessible mask data**. In this representation, earlier tokens mainly correspond to coarse locations and prototypes, while later tokens focus more on local fine-grained details. Each mask token is tightly conditioned on the preceding ones. Hence, this hierarchical design aligns seamlessly with the autoregressive principle of LLMs. By considering **mask tokens as a new language**, it enables LLMs to conveniently gain native segmentation capabilities **without external segmentation foundation models**. As shown in Fig. 2 (c), LLM generates discrete mask tokens just as the way for text tokens, and the final segmentation mask is obtained by de-tokenizing the mask tokens.

We devise a three-stage training recipe to progressively integrate image segmentation capabilities into an LLM. Initially, our HiMTok is trained on a mask image reconstruction task. In the second stage, the LLM and HiMTok are trained together to align visual and language features, utilizing low-resolution images for efficiency. Finally, the LLM is fine-tuned with high-resolution images to adapt to more general scenarios. Additionally, we introduce a Hierarchical Mask Loss (HML) to facilitate the learning of hierarchical mask tokens, providing explicit supervision across different levels of granularity. We also incorporate a bidirectional information flow between mask tokens and box coordinates within the LLM during training.

Through extensive experiments, our method achieves state-of-the-art performance on image segmentation tasks, including referring expression segmentation, reasoning segmentation and open-vocabulary segmentation. Our model also improves referring expression comprehension, a visual grounding task. These results demonstrate the effectiveness of our elegant HiMTok for multi-task learning in LLM. Meanwhile, our competitive performance in general image understanding tasks indicates that HiMTok enables LLMs

to acquire segmentation capabilities without compromising the general abilities.

Succinctly, our contributions are as follows.

- We propose HiMTok, an efficient hierarchical mask tokenizer capable of representing a mask image using up to 32 hierarchical tokens. LMMs are able to learn such token sequences for effective image segmentation, without the need for an image-conditioned mask decoder or off-the-shelf segmentation foundation models.
- A three-stage training recipe and a hierarchical mask loss are devised to ensure the progressive learning of HiMTok and LMM. Bidirectional information flow between segmentation and detection is incorporated for the LMM training.
- Extensive experiments demonstrate that LMM equipped with HiMTok not only shows superiority in various image segmentation tasks, but also improves visual grounding and maintains the general image understanding capability. Interestingly, visual chain-of-thought by “outputting mask tokens before box” improves visual grounding.

## 2. Related Works

Large multimodal models (LMMs) have recently become a popular topic. We have witnessed the continuous improvement in tasks such as visual understanding, OCR, and visual grounding [11, 16, 30, 53, 57, 62, 69]. However, as another fundamental visual task, image segmentation [86] has not been widely included in the capabilities of these open-source large models. In this section, we will review works on image segmentation paradigms in Fig. 2 (a) (b) and image tokenization, to better understand our method.

**Image segmentation with boundary points.** Some works regard segmentation masks as polygons, which makes the image segmentation task similar to sequence-to-sequence object detection that generates box coordinates autoregressively [5, 6, 56, 68, 70]. Early transformer encoder-decoder models [7, 37, 83] have proved the feasibility of using boundary points. LLaFS [84] makes use of LLMs in few-shot segmentation, and exploits a refinement network (similar to Mask2Former [14]) after getting a 16-point polygon from LLM. VistaLLM [44] devises an adaptive sampling strategy to better serialize segmentation masks as points for autoregressive mask generation. This representation struggles with complex shapes and multi-region segmentation.

**Image segmentation with LMM hidden states.** To bring the power of LLMs to image segmentation tasks, LISA [27] introduces a shared special <SEG> token to abstract the feature of interest that further prompt an additional segmentation foundation model (e.g., SAM [26]) to produce the final mask. GSVA [63], LISA++ [67] and LaSagnA [60] expand the number of <SEG> tokens to segment multiple objects. PixelLM [49] incorporates several special

tokens to represent multiple granularities and more targets, and designs a lightweight pixel decoder (similar to SAM [26]). PSALM [78] incorporates a well-designed input schema and uses a powerful segmentation decoder following Mask2Former [14] to improve task generalization. OMG-LLaVA [76] integrates OMG-Seg [31] and an LLM into an end-to-end trainable framework for image understanding and pixel-level reasoning. These methods manage to adapt the strong reasoning ability of LMMs to the mask decoder, *i.e.*, taking hidden states from LLM as continuous prompts to enable an image-conditioned pixel decoder to segment the objects.

**Image tokenization** has been widely explored and applied in visual autoregressive generation. Many works encode images into 2D discrete token grids [17, 46, 48, 55], which are then flattened into sequences for image generation [29, 71]. VAR [54] reformulates visual autoregressive generation as coarse-to-fine next-scale prediction. At each scale, the 2D token grid is predicted simultaneously. Recently, TiTok [74] manages to tokenize a natural image into a few discrete 1D tokens (e.g. 32) in a more compact latent space, which is more efficient. In our method, we regard a segmentation mask as a special image that is represented as a sequence of 1D coarse-to-fine discrete tokens.

## 3. Methodology

### 3.1. Overview

We propose HiMTok, which uses up to 32 hierarchical 1D tokens to efficiently represent segmentation masks for large language models (LLMs), enabling tokenization and reconstruction of masks. Together with the lightweight Mask De-tokenizer, LMMs are enabled to elegantly learn object segmentation, with mask tokens functioning like a new language, as shown in Fig. 2 (c).

To this end, we design a three-stage training recipe for progressive and efficient learning (Fig. 3). HiMTok is first fully trained to enable the single-modality mask tokenization and de-tokenization. In stage 2, the joint training of LMM and HiMTok is performed, which brings vision-language alignment in mask tokenization, while still being efficient with images of low resolution. In stage 3, we focus solely on finetuning the LMM with high-resolution images.

### 3.2. Hierarchical Mask Tokenizer

HiMTok consists of three components: a mask tokenizer (MT), a vector quantization layer (VQ), and a mask de-tokenizer (MD), as illustrated in Fig. 3 (a). Following TiTok [74], some 1D learnable latent tokens are encoded by MT along with mask image patches. After quantized by a VQ variant [85], the encoded latent tokens are then reconstructed by MD\*. The number of 1D mask tokens is much

\*MT and MD are both standard Transformer layers

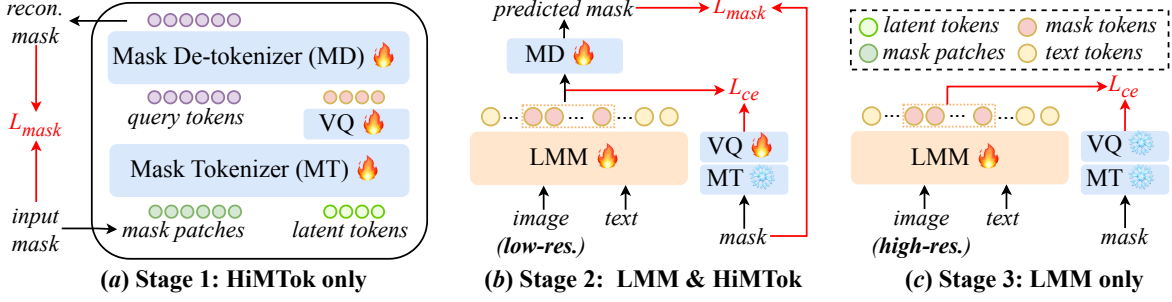


Figure 3. An overview of HiMTok and the 3-stage training recipe. (a) The proposed HiMTok is fully trained in stage 1 by the mask reconstruction task. The VQ loss is emitted here for simplicity. During training, MD takes as input mask tokens of different levels for the hierarchical mask loss. (b) The joint training of LMM and parts of HiMTok in stage 2. Images of low-resolution are used as input for efficiency. The cross entropy loss on text tokens is emitted here. (c) In stage 3, only the LMM is trained with high-resolution images, which is as simple as common LMM training.

smaller than the number of 2D mask patches.

We focus on the hierarchical design here. Hierarchical tokens are expected to carry coarse-to-fine mask representations, which can be implemented by autoregressive modeling [54]. Considering the assumption of unidirectional dependency, we design a causal attention mechanism for the latent tokens in the attention layers of the mask tokenizer: the current latent token is conditioned on the mask patches and its former latent tokens. This mechanism in the mask tokenizer aligns with LLM generation:

$$p(m_1, \dots, m_K | \mathcal{M}) = \prod_{k=1}^K p(m_k | \mathcal{M}, m_1, \dots, m_{k-1}), \quad (1)$$

where  $\mathcal{M}$  is the input mask, and  $m_k$  is the  $k$ -th mask token,  $K$  is the number of mask tokens to represent a mask. Note that the attention between the input mask patches is bidirectional.

**Hierarchical mask loss.** Explicit supervision on mask tokens of different levels is necessary to ensure hierarchy. At the  $l$ -th hierarchical level, the first  $l$  mask tokens are de-tokenized to  $\hat{M}^{(l)}$  independently. In the full level, all mask tokens are used. Based on our observation, few tokens (e.g., 4) usually lead to coarse Gaussian distributions appearing in the mask image after the mask de-tokenizer. Thus, we empirically exploit the Gaussian blur with different sizes of Gaussian kernel on different levels for multi-grained mask label ( $M^{(l)}$ ) preparation. Details on how we make coarse mask labels are illustrated in Appendix B. The hierarchical mask loss (HML) is calculated across the different levels:

$$\mathcal{L}_{mask} = \sum_l \mathcal{L}_{mask}^{(l)}(\hat{M}^{(l)}, M^{(l)}), \quad (2)$$

where  $\mathcal{L}_{mask}^{(l)}$  is the mask loss on the  $l$ -th level that includes a binary cross entropy loss and a Dice loss [52]. In practice,

besides the full level, we sample only a part of other levels following the inverse power-law distribution for the mask loss to train efficiently.

After stage-1 training, HiMTok learns to tokenize segmentation masks into 1D hierarchical tokens in the single mask image modality.

### 3.3. Mask-aware Large Multimodal Model

Regarding the mask tokens in HiMTok as a new language, we can easily incorporate image segmentation capabilities into LMMs. The only modification required for LMM is an expanded vocabulary with the mask token codebook.

**Prompt format.** To highlight and distinguish the segmentation task and mask tokens from natural language, we exploit some special tokens to indicate them. Simply put, we use “<ref>referred object</ref>” to pinpoint the object to be segmented, and <mt\_start>mt.i ... <mt\_end> to indicate the segmentation mask tokens. Besides, visual grounding is also involved in our experiments as a regular vision-language task, where we use “<box>[x1, y1, x2, y2]</box>” to indicate the bounding box. More details about the prompt design are listed in Appendix I.

**Bidirectional information flow.** Detection and segmentation are two classic tasks for object locating. To learn the inherent relation between masks and bounding boxes, we incorporate bidirectional information flow into our training data, i.e., both box-to-mask and mask-to-box token orders are considered. LMM is expected to output corresponding mask tokens given a bounding box, and vice versa. The bounding boxes are generated directly by LMM rather than derived from parsing the de-tokenized masks. This approach allows the LLM to achieve good consistency and performance in learning detection and segmentation tasks.

**Progressive training.** To enable LMM to learn mask tokens while maintaining its general capability, we train LMM in two stages, as shown in Fig. 3 (b) (c). In stage 2, a mas-



sive amount of image segmentation data is used along with some general data. The mask tokenization is aligned with vision-language through joint training. Since the LMM encounters various segmentation cases, the understanding of mask tokens is gradually improved. Low-resolution images are used to train effectively. Both the cross entropy loss ( $L_{ce}$ ) for next-token-prediction and the hierarchical mask loss are adopted for optimization. In stage 3, the LMM is further trained with high-resolution images as input. The amount of segmentation data is reduced to avoid collapse on the general capacity. Only the cross entropy loss is used.

**Inference.** During inference, if mask tokens are detected in the LLM output, the lightweight mask de-tokenizer will visualize them as the final predicted segmentation mask. Alternatively, the mask from our de-tokenizer can be further potentially refined by feeding it into an independently finetuned SAM [26]. Details on SAM finetuning for optional usage can be found in Appendix C. We do not utilize SAM in our experiments by default, unless explicitly stated.

## 4. Experiments

### 4.1. Training Datasets

Since the LMM is expected to learn brand-new mask tokens for image segmentation while maintaining its original capability, both segmentation data and general-purpose data are necessary for effective training. All datasets transcribed in the 3 stages are listed in Tab. 1. For stage-1 training, we exploit the groundtruth masks in all the segmentation-related datasets to train our HiMTok. Random cropping is adopted to augment the binary mask images. For stage 2, all the listed datasets are used with a total amount of 7.1 million. The ratio of segmentation data reaches up to 0.41, which accelerates the learning of mask tokens. For stage 3, we discard a large number of segmentation and detection samples that are low-quality or overly simplistic in instruction. The details of the down-sampled datasets are listed in Appendix D. As a result, the total amount of training data is decreased to 5.0 million, with the ratio of segmentation data dropping to 0.24, which ensure the general performance.

### 4.2. Implementation Details

In stage 1, HiMTok is initialized with TiTok-L-32 [74]. The resolution of input and reconstructed mask is  $256 \times 256$ . We use 32 latent tokens to represent a mask image with the codebook size of 1024. When calculating the hierarchical mask loss, we use 4 levels of mask tokens, including one full-level and three sampled partial levels. In stage 2, InternVL 2.5 [11] is chosen as the LMM. The input image size is the base resolution  $448 \times 448$ . In stage 3, we support high-resolution input images.

Table 1. Training data. \* (.) means the dataset is partly sampled. Datasets with # are for Mask Perception (Appendix E). † means the dataset is synthesized using the open-source engine.

Key Token	Task	Datasets
Mask (2.9M)	Sem./Inst. Seg.	ADE20K [81], PASCAL Context [42], PartImageNet [22], LVIS-PACO [45], COCO-Rem [51], COCO-Stuff [4], COCO-Panoptic [33]
	Prompt Seg.	SA1B* (1M) [26]
	RES	RefCOCO+/g [40, 72], gRefCOCO [34], refCLEF [24]
	Reason Seg.	LISA++ Inst. Seg. & CoT [67]
	Mask Perception	RefCOCO+/g# [40, 72], gRefCOCO# [34]
Coordinate (0.5M)	Object Det.	Objects365* (450K) [50]
	REC	Cops-Ref [9], SK-VG [10]
	Referential Dialogue	BoxCoT [5]
Text (3.7M)	Caption	InternVL-SA1B-Caption [12], ALLaVA-Caption-LAION-4V [21]
	VQA	LLaVA-150K [35], VQAv2 [20], ALLaVA-Instruct [21], GQA [23], DOCCI [43], CogVLMSFT [59], SVIT [79], SynthClock† [66], AI2D [25], MMInstruct* (222K) [38], Cauldron* (234K) [28]
	NLP	Evol-Instruct [21], Dolly [15], Code-Feedback [80], MathInstruct [75], MetaMathQA [73], Orca-Math [41]

### 4.3. Referring Expression Segmentation

Referring Expression Segmentation (RES) is a representative task for evaluation of language-guided segmentation. We test two versions of our model: one is trained with the 3 stages, the other is further finetuned on the RefCOCO+/g training set and a small ratio (around 0.3) of mixed general data. Three classic benchmarks, RefCOCO+/g [40, 72], are used to evaluate our method. As shown in Tab. 2, LMM equipped with HiMTok (LMM<sub>HiMTok</sub>-8B) achieves competitive performance without task-specific finetuning and any Segmentation Foundation Models (SFM). After finetuning, our SFM-free method achieves state-of-the-art performance on all three benchmarks, which not only significantly outperforms previous SFM-free methods, but also beats those with SFM. Optionally, we obtain further improvement by feeding the mask from our de-tokenizer into a finetuned SAM [26]. The superiority is more significant on RefCOCO+/g where text semantics are more challenging for segmentation, which is owed to the unified modeling of language and segmentation in LMM.

We also evaluate on gRefCOCO [34], a benchmark for

Table 2. Results (cIoU) on the RES benchmarks (RefCOCO+/g). SFM denotes Segmentation Foundation Models or similar modules, either original or finetuned. “(ft)” means the model is finetuned on the in-domain training set.

Paradigm	Method	w/ SFM	RefCOCO			RefCOCO+			RefCOCog	
			val	testA	testB	val	testA	testB	val(U)	test(U)
Boundary Point-based	PolyFormer-B [37]	×	74.8	76.6	71.1	67.6	72.9	59.3	67.8	69.1
	VistaLLM-7B [44]	×	74.5	76.0	72.7	69.1	73.7	64.0	69.0	70.9
Hidden State-based	LISA-7B(ft) [27]	✓	74.9	79.1	72.3	65.1	70.8	58.1	67.9	70.6
	PixelLM-7B [49]	✓	73.0	76.5	68.2	66.3	71.7	58.3	69.3	70.5
	GSVA-7B [63]	✓	76.4	77.4	72.8	64.5	67.7	58.6	71.1	72.0
	GSVA-7B(ft) [63]	✓	77.2	78.9	73.5	65.9	69.6	59.8	72.7	73.3
	LaSagnA-7B [60]	✓	76.8	78.7	73.8	66.4	70.6	60.1	70.6	71.9
	VisionLLM v2 [61]	✓	76.6	79.3	74.3	64.5	69.8	61.5	70.7	71.2
	OMG-LLaVA [76]	✓	75.6	77.7	71.2	65.6	69.7	58.9	70.7	70.2
	OMG-LLaVA(ft) [76]	✓	78.0	80.3	74.1	69.1	73.1	63.0	72.9	72.9
	GLaMM [47]	✓	79.5	83.2	76.9	72.6	78.7	64.6	74.2	74.9
	u-LLaVA [64]	✓	83.0	85.1	80.5	77.1	81.7	70.6	77.1	78.0
	PSALM [78]	✓	83.6	84.7	81.6	72.9	75.5	70.1	73.8	74.4
Others	GroundHog-7B [77]	✓	78.5	79.9	75.7	70.5	75.0	64.9	74.1	74.6
	SAM4MLLM-8B [8]	✓	79.8	82.7	74.7	74.6	80.0	67.2	75.5	76.4
Mask Token-based	LMM <sub>HiMTok</sub> -8B	×	81.1	81.2	79.2	77.1	78.8	71.5	75.8	76.7
	LMM <sub>HiMTok</sub> -8B(ft)	×	<b>85.0</b>	<b>85.2</b>	<b>83.5</b>	<b>79.7</b>	<b>82.7</b>	<b>76.0</b>	<b>80.0</b>	<b>80.6</b>
	LMM <sub>HiMTok</sub> -8B(ft) + SAM	✓	<b>85.9</b>	<b>86.3</b>	<b>83.9</b>	<b>80.5</b>	<b>83.7</b>	<b>76.4</b>	<b>80.1</b>	<b>80.9</b>

Table 3. Results on generalized referring expression segmentation. \* indicates zero-shot performance.

Method	val		testA		testB	
	cIoU	gIoU	cIoU	gIoU	cIoU	gIoU
LISA-7B[27]	38.7	32.2	52.6	48.5	44.8	39.7
LISA-7B(ft)[27]	61.8	61.6	68.5	66.3	60.6	58.8
GSVA-7B[63]	61.7	63.3	69.2	70.1	60.3	61.3
GSVA-7B(ft)[63]	63.3	66.5	69.9	71.1	60.5	62.2
LaSagnA* [60]	38.1	32.4	50.4	47.3	42.1	38.9
PSALM* [78]	42.0	43.3	52.4	54.5	50.6	52.5
GroundHog-7B [77]	-	66.7	-	-	-	-
SAM4MLLM-8B [8]	67.8	71.9	72.2	<b>74.2</b>	63.4	65.3
LMM <sub>HiMTok</sub> -8B	66.8	68.7	68.6	67.6	65.8	64.1
LMM <sub>HiMTok</sub> -8B(ft)	<b>70.4</b>	<b>72.1</b>	<b>74.9</b>	73.5	<b>72.0</b>	<b>71.7</b>

Generalized Referring Expression Segmentation (GRES) that poses challenges in referring to multiple or no objects. Specifically, we first ask our model whether the object exists. The segmentation instruction is assigned only when the first response is “yes”. Tab. 3 lists the results on gRefCOCO. Similar conclusions can be observed. Previous hidden state-based LMMs rely much on SFM, which may restrict the upper bound of their performance on segmenting multiple objects or reject non-existence segmentation.

#### 4.4. Reasoning Segmentation

Our method can segment objects given complex and implicit instructions. Inspired by CoReS [2], we design a CoT strategy to generate segmentation masks progressively. Our model is prompted to answer the question with text first and then perform segmentation on the answered objects.

As shown in Tab. 4, our method achieves the best per-

formance with the previous SOTA of similar model size in ReasonSeg [27], a benchmark featuring complicated and obscure instructions. Notably, our scores on both the validation and test sets are nearly identical, whereas other methods show lower performance on the test set, which contains a large proportion of short and sophisticated questions. This further demonstrates that our model not only possesses strong segmentation capabilities but also retains powerful text understanding.

#### 4.5. Open-vocabulary Segmentation

Our LMM equipped with HiMTok performs well not only in-domain but also out-of-domain. We evaluated our model on open-vocabulary segmentation benchmarks, including ADE20K (A-150) [82], PASCAL Context59 (PC-59) [42], and PASCAL VOC 20 (PAS-20) [18]. The large number of defined classes is disadvantageous for our method. Previous segmentation models have typically approached this by either inputting all categories simultaneously for joint modeling or by treating the task as a dense classification problem, resulting in mutual exclusivity between categories. The semantic similarity of some class names can lead to confusion for models that have not been specifically trained to handle such nuances.

We do not feed all the classes into our model to avoid lengthy token sequence and over-finetuning. Instead, each question contains only one class. Since many classes do not exist in a single image, we first ask whether the object exists, as we do in gRefCOCO. Masks of different categories may overlap due to the ambiguity of class names and er-

Table 4. Results on ReasonSeg.

Method	val		test	
	gIoU	cIoU	gIoU	cIoU
LISA-7B[27]	44.4	46.0	36.8	34.1
LISA-7B(ft)[27]	52.9	54.0	47.3	48.4
GroundHog-7B [77]	56.2	-	-	-
VisionLLM v2 [61]	51.0	-	-	-
LaSagnA [60]	48.8	47.2	-	-
VISA-7B [65]	52.7	57.8	-	-
SAM4MLLM-8B [8]	58.4	60.4	-	-
CoReS-7B [2]	59.4	-	52.4	-
LMM <sub>HiMTok</sub> -8B	<b>60.7</b>	<b>67.0</b>	<b>60.8</b>	<b>66.2</b>

Table 5. Results (mIoU) on open-vocabulary segmentation.

Method	A-150	PC-59	PAS-20
LaSagnA [60]	14.3	46.1	69.8
PSALM [78]	18.2	<b>48.5</b>	81.3
LMM <sub>HiMTok</sub> -8B	<b>25.0</b>	43.9	<b>82.0</b>

ror from the model. We empirically prioritize assigning the category of the mask with the smaller area to the confused pixel if several classes are predicted.

As shown in Tab. 5, our method achieves the best scores in A-150 and PAS-20, while competitive in PC-59. General language capability of LMM<sub>HiMTok</sub> plays a key role in understanding open-vocabulary class names, which is well generalized to the segmentation task.

#### 4.6. Referring Expression Comprehension

Here we present the results on the REC benchmarks, which are widely recognized for visual grounding evaluation. Our output boxes are generated directly by the LMM following the mask tokens, without any post-processing based on segmentation masks. This approach is highly efficient if our goal is solely object detection, as it bypasses the de-tokenization process.

As illustrated in Tab. 6, our method significantly outperforms previous general segmentation models as well as our baseline model, the robust InternVL2.5-8B. This indicates that detection is enhanced through joint training with segmentation. The effect of mask token length on REC is studied in Sec. 4.8.1.

#### 4.7. General Image Understanding

After learning image segmentation, our model continues to maintain its comprehensive image understanding capabilities, which is crucial.

We compare our model with the baseline on MME [19]. As in Tab. 7, our model is comparable to InternVL2.5-8B across various dimensions. The joint learning of segmentation even brings some promotion in image understanding of some areas, *e.g.*, position, scene. However, the performance drops in some dimensions, which is due to the lack of

Table 6. Results on the REC benchmarks. Acc@0.5 is reported.

Method	RefCOCO			RefCOCO+			RefCOCOg	
	val	testA	testB	val	testA	testB	val	test
LISA-7B(ft) [27]	85.4	88.8	82.6	74.2	79.5	68.4	79.3	80.4
GSVA-7B(ft) [63]	86.3	89.2	83.8	72.8	78.8	68.0	81.6	81.8
u-LLaVA [64]	86.0	89.5	82.3	74.1	81.2	66.7	79.9	81.7
InternVL2.5-8B	90.3	94.5	85.9	85.2	91.5	78.8	86.7	87.6
LMM <sub>HiMTok</sub> -8B	<b>92.9</b>	<b>94.7</b>	<b>89.3</b>	<b>87.6</b>	<b>91.5</b>	<b>81.5</b>	<b>88.5</b>	<b>89.0</b>

Table 7. Results on part of dimensions in MME.

Method	existence	count	position	color	posters	celebrity	scene
InternVL2.5-8B	<b>200</b>	<b>170</b>	163	<b>180</b>	<b>169</b>	<b>140</b>	154
LMM <sub>HiMTok</sub> -8B	<b>200</b>	160	<b>166</b>	<b>180</b>	164	132	<b>163</b>
LMM <sub>HiMTok</sub> -8B (ft)	190	113	120	153	57	81	157

diverse and high-quality data in this segmentation-oriented version. For example, we do not specially incorporate data on celebrity and OCR. This also explains why the performance of LMM<sub>HiMTok</sub>(ft) differs significantly across the dimensions: the segmentation data we used has stronger bias on existence and scene than others. The model retains intrinsic semantic understanding, despite being fine-tuned exclusively on segmentation data. More results on the general image understanding are listed in Appendix G.

#### 4.8. Ablation Study

##### 4.8.1. Effect of the mask token length

Mask tokens of different lengths correspond to different granularities for mask representation. We investigate the effect of mask token length on segmentation (RES) and detection (REC) respectively.

Considering that our model was trained with full-length ( $K$  in Eq. (1)) mask token sequences, we finetune it using a mixture of token sequences with varying lengths, by specifying the length in the prompt. Details on the prompt format can be found in Appendix I. We evaluate on the RefCOCO validation set.

The effect on RES is shown in Fig. 4. As the mask token length increases, cIoU improves while the gains gradually taper off. With 16 mask tokens, our method has already achieved 82.8% cIoU. By further expanding the token length to 32, we get additional 2.5% cIoU improvement. As shown in the right column of Fig. 5, the fine-grained details become more accurate with longer mask token length. For simple shapes or less strict scenarios, 16 tokens are enough for representation.

For REC, the object bounding box is predicted after mask tokens of varying lengths. It is exactly a kind of visual chain-of-thought. We report accuracy on 3 IoU thresholds: 0.5, 0.7 and 0.9, which correspond to evaluations of varying levels from coarse to fine. Fig. 5 shows the effect on REC. As the role segmentation plays, more mask tokens contribute to more refined box prediction. As more mask tokens are used, acc@0.5 sees a slight improvement, while acc@0.9 improves significantly. These findings prove the

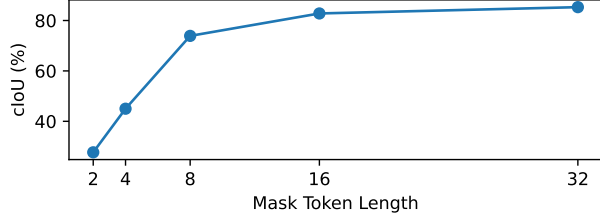


Figure 4. The effect of mask token length on RES. The RefCOCO validation set is used.

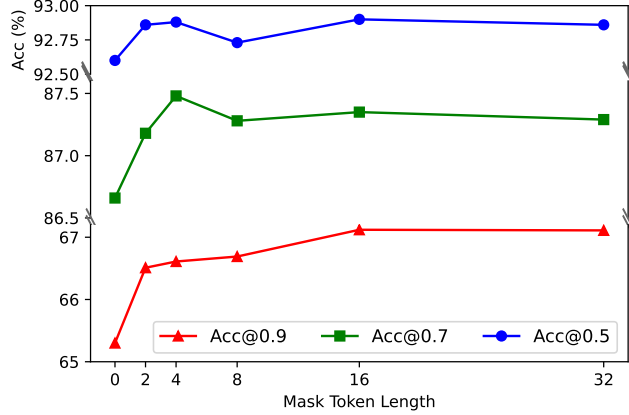


Figure 5. The effect of mask token length on REC with different IoU thresholds. The RefCOCO validation set is used. Note that the acc dimension is not continuous.

information flow from mask tokens to box coordinates is very useful in both training and evaluation phase. From some perspective, we can regard the hierarchical mask tokens as a chain-of-thought for visual grounding. By the way, we do not see improvement on RES for the information flow from box to mask. This may be due to the fact that the former mask tokens are easier to generate than the direct box coordinates.

#### 4.8.2. Effect of hierarchical mask loss

The hierarchical mask loss (HML) is vital for the coarse-to-fine representation learning. To verify this, we perform 3-stage training without HML. Instead, the mask loss  $\mathcal{L}_{mask}$  consists solely of the full-level mask supervision.

We observe a significant performance degradation without HML. As shown in Tab. 8, RefCOCO+/g, where expression understanding is emphasized, experiences a substantial drop, while RefCOCO shows a relatively minor decline. We speculate that mask token learning during training without HML compromised the model’s general capability. Without HML, mask tokens may be learned through shortcuts, and the redundancy within the 32 tokens increases the learning difficulty, potentially disrupting the acquisition and retention of general understanding.

As shown on the left of Fig. 6, mask tokens fewer than 32 lead to completely incorrect segmentation masks, which

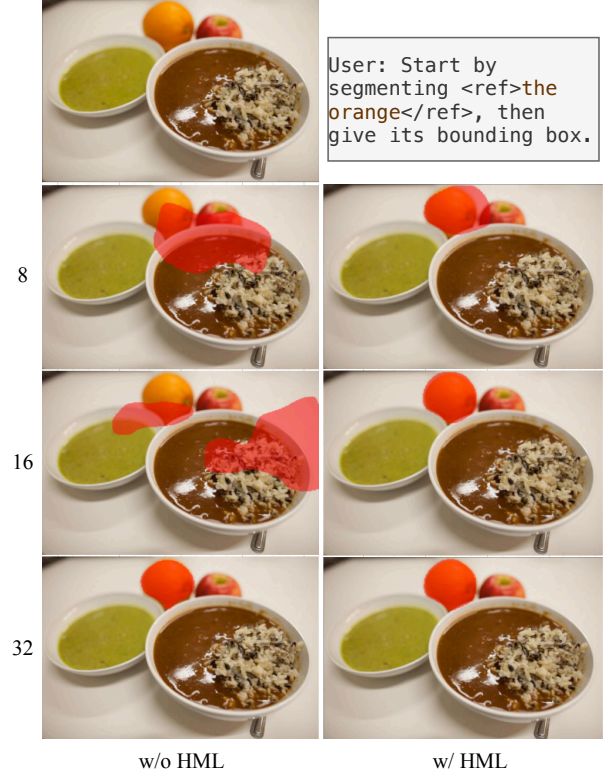


Figure 6. An example that illustrates the effect of different mask token length (8, 16, 32) for our model trained with and without HML. For model without using HML, full tokens are restrictly required for the mask quality, while model with HML can segment simple objects with fewer tokens.

Table 8. Ablation on the hierarchical mask loss (HML). The validation set is used for comparison.

HML	RefCOCO	RefCOCO+	RefCOCOg
×	79.2	64.7	63.9
✓	<b>81.1</b>	<b>77.1</b>	<b>75.8</b>

suggests that training without HML strictly requires the use of full-length mask tokens throughout. In contrast, the use of our hierarchical mask tokens is flexible. More interesting visualization cases are presented in Appendix H.

## 5. Conclusion

We present HiMTok, a Hierarchical Mask Tokenizer that represents segmentation masks as hierarchical mask token sequences. Existing LMMs equipped with HiMTok are capable of learning to segment objects specified by language prompts. Hierarchical mask loss is proposed to ensure the learning of coarse-to-fine mask tokens. We also develop a 3-stage training recipe for progressive learning of segmentation and general visual capabilities. Extensive experiments demonstrate the effectiveness of HiMTok in a variety of visual and segmentation tasks.



## References

- [1] Jinze Bai, Shuai Bai, Shusheng Yang, Shijie Wang, Sinan Tan, Peng Wang, Junyang Lin, Chang Zhou, and Jingren Zhou. Qwen-vl: A versatile vision-language model for understanding, localization, text reading, and beyond. *arXiv preprint arXiv:2308.12966*, 2023. 1
- [2] Xiaoyi Bao, Siyang Sun, Shuailei Ma, Kecheng Zheng, Yuxin Guo, Guosheng Zhao, Yun Zheng, and Xingang Wang. Cores: Orchestrating the dance of reasoning and segmentation. In *European Conference on Computer Vision*, pages 187–204. Springer, 2024. 2, 6, 7
- [3] Amir Bar, Yossi Gandelsman, Trevor Darrell, Amir Globerson, and Alexei Efros. Visual prompting via image inpainting. *Advances in Neural Information Processing Systems*, 35:25005–25017, 2022. 2
- [4] Holger Caesar, Jasper Uijlings, and Vittorio Ferrari. Cocosuff: Thing and stuff classes in context. In *Proceedings of the IEEE conference on computer vision and pattern recognition*, pages 1209–1218, 2018. 5
- [5] Keqin Chen, Zhao Zhang, Weili Zeng, Richong Zhang, Feng Zhu, and Rui Zhao. Shikra: Unleashing multimodal llm’s referential dialogue magic. *arXiv preprint arXiv:2306.15195*, 2023. 3, 5
- [6] Ting Chen, Saurabh Saxena, Lala Li, David J Fleet, and Geoffrey Hinton. Pix2seq: A language modeling framework for object detection. *arXiv preprint arXiv:2109.10852*, 2021. 3
- [7] Ting Chen, Saurabh Saxena, Lala Li, Tsung-Yi Lin, David J Fleet, and Geoffrey E Hinton. A unified sequence interface for vision tasks. *Advances in Neural Information Processing Systems*, 35:31333–31346, 2022. 1, 3
- [8] Yi-Chia Chen, Wei-Hua Li, Cheng Sun, Yu-Chiang Frank Wang, and Chu-Song Chen. Sam4mllm: Enhance multimodal large language model for referring expression segmentation. In *European Conference on Computer Vision*, pages 323–340. Springer, 2024. 6, 7
- [9] Zhenfang Chen, Peng Wang, Lin Ma, Kwan-Yee K Wong, and Qi Wu. Cops-ref: A new dataset and task on compositional referring expression comprehension. In *Proceedings of the IEEE/CVF Conference on Computer Vision and Pattern Recognition*, pages 10086–10095, 2020. 5
- [10] Zhihong Chen, Ruifei Zhang, Yibing Song, Xiang Wan, and Guanbin Li. Advancing visual grounding with scene knowledge: Benchmark and method. In *Proceedings of the IEEE/CVF Conference on Computer Vision and Pattern Recognition*, pages 15039–15049, 2023. 5
- [11] Zhe Chen, Weiyun Wang, Yue Cao, Yangzhou Liu, Zhangwei Gao, Erfei Cui, Jinguo Zhu, Shenglong Ye, Hao Tian, Zhaoyang Liu, et al. Expanding performance boundaries of open-source multimodal models with model, data, and test-time scaling. *arXiv preprint arXiv:2412.05271*, 2024. 3, 5, 4
- [12] Zhe Chen, Weiyun Wang, Hao Tian, Shenglong Ye, Zhangwei Gao, Erfei Cui, Wenwen Tong, Kongzhi Hu, Jiapeng Luo, Zheng Ma, et al. How far are we to gpt-4v? closing the gap to commercial multimodal models with open-source suites. *Science China Information Sciences*, 67(12):220101, 2024. 5
- [13] Zhe Chen, Jiannan Wu, Wenhai Wang, Weijie Su, Guo Chen, Sen Xing, Muyan Zhong, Qinglong Zhang, Xizhou Zhu, Lewei Lu, et al. Internvl: Scaling up vision foundation models and aligning for generic visual-linguistic tasks. In *Proceedings of the IEEE/CVF Conference on Computer Vision and Pattern Recognition*, pages 24185–24198, 2024. 1
- [14] Bowen Cheng, Ishan Misra, Alexander G Schwing, Alexander Kirillov, and Rohit Girdhar. Masked-attention mask transformer for universal image segmentation. In *Proceedings of the IEEE/CVF conference on computer vision and pattern recognition*, pages 1290–1299, 2022. 2, 3
- [15] Mike Conover, Matt Hayes, Ankit Mathur, Jianwei Xie, Jun Wan, Sam Shah, Ali Ghodsi, Patrick Wendell, Matei Zaharia, and Reynold Xin. Free dolly: Introducing the world’s first truly open instruction-tuned llm, 2023. 5
- [16] Abhimanyu Dubey, Abhinav Jauhri, Abhinav Pandey, Abhishek Kadian, Ahmad Al-Dahle, Aiesha Letman, Akhil Mathur, Alan Schelten, Amy Yang, Angela Fan, et al. The llama 3 herd of models. *arXiv preprint arXiv:2407.21783*, 2024. 1, 3
- [17] Patrick Esser, Robin Rombach, and Bjorn Ommer. Taming transformers for high-resolution image synthesis. In *Proceedings of the IEEE/CVF conference on computer vision and pattern recognition*, pages 12873–12883, 2021. 2, 3
- [18] Mark Everingham, Luc Van Gool, Christopher KI Williams, John Winn, and Andrew Zisserman. The pascal visual object classes (voc) challenge. *International journal of computer vision*, 88:303–338, 2010. 6
- [19] Chaoyou Fu, Peixian Chen, Yunhang Shen, Yulei Qin, Mengdan Zhang, Xu Lin, Jinrui Yang, Xiawu Zheng, Ke Li, Xing Sun, et al. Mme: A comprehensive evaluation benchmark for multimodal large language models. *arXiv preprint arXiv:2306.13394*, 2023. 7, 3
- [20] Yash Goyal, Tejas Khot, Douglas Summers-Stay, Dhruv Batra, and Devi Parikh. Making the v in vqa matter: Elevating the role of image understanding in visual question answering. In *Proceedings of the IEEE conference on computer vision and pattern recognition*, pages 6904–6913, 2017. 5, 3
- [21] Guiming Hardy Chen, Shunian Chen, Ruifei Zhang, Junying Chen, Xiangbo Wu, Zhiyi Zhang, Zhihong Chen, Jianquan Li, Xiang Wan, and Benyou Wang. Allava: Harnessing gpt4v-synthesized data for a lite vision-language model. *arXiv e-prints*, pages arXiv–2402, 2024. 5
- [22] Ju He, Shuo Yang, Shaokang Yang, Adam Kortylewski, Xiaoding Yuan, Jie-Neng Chen, Shuai Liu, Cheng Yang, Qihang Yu, and Alan Yuille. Partimagenet: A large, high-quality dataset of parts. In *European Conference on Computer Vision*, pages 128–145. Springer, 2022. 5
- [23] Drew A Hudson and Christopher D Manning. Gqa: A new dataset for real-world visual reasoning and compositional question answering. In *Proceedings of the IEEE/CVF conference on computer vision and pattern recognition*, pages 6700–6709, 2019. 5
- [24] Sahar Kazemzadeh, Vicente Ordonez, Mark Matten, and Tamara Berg. Referitgame: Referring to objects in photographs of natural scenes. In *Proceedings of the 2014 conference on empirical methods in natural language processing (EMNLP)*, pages 787–798, 2014. 5

- [25] Aniruddha Kembhavi, Mike Salvato, Eric Kolve, Minjoon Seo, Hannaneh Hajishirzi, and Ali Farhadi. A diagram is worth a dozen images. In *Computer Vision–ECCV 2016: 14th European Conference, Amsterdam, The Netherlands, October 11–14, 2016, Proceedings, Part IV 14*, pages 235–251. Springer, 2016. 5
- [26] Alexander Kirillov, Eric Mintun, Nikhila Ravi, Hanzi Mao, Chloe Rolland, Laura Gustafson, Tete Xiao, Spencer Whitehead, Alexander C Berg, Wan-Yen Lo, et al. Segment anything. In *Proceedings of the IEEE/CVF International Conference on Computer Vision*, pages 4015–4026, 2023. 2, 3, 5, 1
- [27] Xin Lai, Zhuotao Tian, Yukang Chen, Yanwei Li, Yuhui Yuan, Shu Liu, and Jiaya Jia. Lisa: Reasoning segmentation via large language model. In *Proceedings of the IEEE/CVF Conference on Computer Vision and Pattern Recognition*, pages 9579–9589, 2024. 1, 2, 3, 6, 7
- [28] Hugo Laurençon, Léo Tronchon, Matthieu Cord, and Victor Sanh. What matters when building vision-language models? *arXiv preprint arXiv:2405.02246*, 2024. 5
- [29] Doyup Lee, Chiheon Kim, Saehoon Kim, Minsu Cho, and Wook-Shin Han. Autoregressive image generation using residual quantization. In *Proceedings of the IEEE/CVF Conference on Computer Vision and Pattern Recognition*, pages 11523–11532, 2022. 3
- [30] Dongxu Li, Yudong Liu, Haoning Wu, Yue Wang, Zhiqi Shen, Bowen Qu, Xinyao Niu, Guoyin Wang, Bei Chen, and Junnan Li. Aria: An open multimodal native mixture-of-experts model. *arXiv preprint arXiv:2410.05993*, 2024. 3
- [31] Xiangtai Li, Haobo Yuan, Wei Li, Henghui Ding, Size Wu, Wenwei Zhang, Yining Li, Kai Chen, and Chen Change Loy. Omg-seg: Is one model good enough for all segmentation? In *Proceedings of the IEEE/CVF Conference on Computer Vision and Pattern Recognition*, pages 27948–27959, 2024. 3
- [32] Yifan Li, Yifan Du, Kun Zhou, Jinpeng Wang, Wayne Xin Zhao, and Ji-Rong Wen. Evaluating object hallucination in large vision-language models. *arXiv preprint arXiv:2305.10355*, 2023. 3
- [33] Tsung-Yi Lin, Michael Maire, Serge Belongie, James Hays, Pietro Perona, Deva Ramanan, Piotr Dollár, and C Lawrence Zitnick. Microsoft coco: Common objects in context. In *Computer vision–ECCV 2014: 13th European conference, zurich, Switzerland, September 6–12, 2014, proceedings, part v 13*, pages 740–755. Springer, 2014. 5
- [34] Chang Liu, Henghui Ding, and Xudong Jiang. Gres: Generalized referring expression segmentation. In *Proceedings of the IEEE/CVF conference on computer vision and pattern recognition*, pages 23592–23601, 2023. 5
- [35] Haotian Liu, Chunyuan Li, Qingyang Wu, and Yong Jae Lee. Visual instruction tuning. *Advances in neural information processing systems*, 36, 2023. 1, 5
- [36] Haotian Liu, Chunyuan Li, Yuheng Li, and Yong Jae Lee. Improved baselines with visual instruction tuning. In *Proceedings of the IEEE/CVF Conference on Computer Vision and Pattern Recognition*, pages 26296–26306, 2024. 1
- [37] Jiang Liu, Hui Ding, Zhaowei Cai, Yuting Zhang, Ravi Kumar Satzoda, Vijay Mahadevan, and R Manmatha. Polyformer: Referring image segmentation as sequential polygon generation. In *Proceedings of the IEEE/CVF Conference on Computer Vision and Pattern Recognition*, pages 18653–18663, 2023. 3, 6
- [38] Yangzhou Liu, Yue Cao, Zhangwei Gao, Weiyun Wang, Zhe Chen, Wenhai Wang, Hao Tian, Lewei Lu, Xizhou Zhu, Tong Lu, et al. Mminstruct: A high-quality multi-modal instruction tuning dataset with extensive diversity. *Science China Information Sciences*, 67(12):1–16, 2024. 5
- [39] Jiasen Lu, Christopher Clark, Rowan Zellers, Roozbeh Mottaghi, and Aniruddha Kembhavi. Unified-io: A unified model for vision, language, and multi-modal tasks. In *The Eleventh International Conference on Learning Representations*, 2022. 2
- [40] Junhua Mao, Jonathan Huang, Alexander Toshev, Oana Camburu, Alan L Yuille, and Kevin Murphy. Generation and comprehension of unambiguous object descriptions. In *Proceedings of the IEEE conference on computer vision and pattern recognition*, pages 11–20, 2016. 5, 2
- [41] Arindam Mitra, Hamed Khanpour, Corby Rosset, and Ahmed Awadallah. Orca-math: Unlocking the potential of slms in grade school math. *arXiv preprint arXiv:2402.14830*, 2024. 5
- [42] Roozbeh Mottaghi, Xianjie Chen, Xiaobai Liu, Nam-Gyu Cho, Seong-Whan Lee, Sanja Fidler, Raquel Urtasun, and Alan Yuille. The role of context for object detection and semantic segmentation in the wild. In *Proceedings of the IEEE conference on computer vision and pattern recognition*, pages 891–898, 2014. 5, 6
- [43] Yasumasa Onoe, Sunayana Rane, Zachary Berger, Yonatan Bitton, Jaemin Cho, Roopal Garg, Alexander Ku, Zarana Parekh, Jordi Pont-Tuset, Garrett Tanzer, et al. Docci: Descriptions of connected and contrasting images. In *European Conference on Computer Vision*, pages 291–309. Springer, 2024. 5
- [44] Shraman Pramanick, Guangxing Han, Rui Hou, Sayan Nag, Ser-Nam Lim, Nicolas Ballas, Qifan Wang, Rama Chellappa, and Amjad Almahairi. Jack of all tasks master of many: Designing general-purpose coarse-to-fine vision-language model. In *Proceedings of the IEEE/CVF Conference on Computer Vision and Pattern Recognition*, pages 14076–14088, 2024. 1, 2, 3, 6
- [45] Vignesh Ramanathan, Anmol Kalia, Vladan Petrovic, Yi Wen, Baixue Zheng, Baishan Guo, Rui Wang, Aaron Marquez, Rama Kovvuri, Abhishek Kadian, et al. Paco: Parts and attributes of common objects. In *Proceedings of the IEEE/CVF Conference on Computer Vision and Pattern Recognition*, pages 7141–7151, 2023. 5
- [46] Aditya Ramesh, Mikhail Pavlov, Gabriel Goh, Scott Gray, Chelsea Voss, Alec Radford, Mark Chen, and Ilya Sutskever. Zero-shot text-to-image generation. In *International conference on machine learning*, pages 8821–8831. Pmlr, 2021. 3
- [47] Hanoona Rasheed, Muhammad Maaz, Sahal Shaji, Abdelrahman Shaker, Salman Khan, Hisham Cholakkal, Rao M Anwer, Eric Xing, Ming-Hsuan Yang, and Fahad S Khan. Glamm: Pixel grounding large multimodal model. In *Proceedings of the IEEE/CVF Conference on Computer Vision and Pattern Recognition*, pages 13009–13018, 2024. 2, 6

- [48] Ali Razavi, Aaron Van den Oord, and Oriol Vinyals. Generating diverse high-fidelity images with vq-vae-2. *Advances in neural information processing systems*, 32, 2019. 3
- [49] Zhongwei Ren, Zhicheng Huang, Yunchao Wei, Yao Zhao, Dongmei Fu, Jiashi Feng, and Xiaojie Jin. Pixellm: Pixel reasoning with large multimodal model. In *Proceedings of the IEEE/CVF Conference on Computer Vision and Pattern Recognition*, pages 26374–26383, 2024. 1, 2, 3, 6
- [50] Shuai Shao, Zeming Li, Tianyuan Zhang, Chao Peng, Gang Yu, Xiangyu Zhang, Jing Li, and Jian Sun. Objects365: A large-scale, high-quality dataset for object detection. In *Proceedings of the IEEE/CVF international conference on computer vision*, pages 8430–8439, 2019. 5
- [51] Shweta Singh, Aayan Yadav, Jitesh Jain, Humphrey Shi, Justin Johnson, and Karan Desai. Benchmarking object detectors with coco: A new path forward. In *European Conference on Computer Vision*, pages 279–295. Springer, 2024. 5
- [52] Carole H Sudre, Wenqi Li, Tom Vercauteren, Sebastien Ourselin, and M Jorge Cardoso. Generalised dice overlap as a deep learning loss function for highly unbalanced segmentations. In *Deep Learning in Medical Image Analysis and Multimodal Learning for Clinical Decision Support: Third International Workshop, DLMIA 2017, and 7th International Workshop, ML-CDS 2017, Held in Conjunction with MICCAI 2017, Québec City, QC, Canada, September 14, Proceedings 3*, pages 240–248. Springer, 2017. 4
- [53] Gemini Team, Petko Georgiev, Ving Ian Lei, Ryan Burnell, Libin Bai, Anmol Gulati, Garrett Tanzer, Damien Vincent, Zhufeng Pan, Shibo Wang, et al. Gemini 1.5: Unlocking multimodal understanding across millions of tokens of context. *arXiv preprint arXiv:2403.05530*, 2024. 3
- [54] Keyu Tian, Yi Jiang, Zehuan Yuan, Bingyue Peng, and Liwei Wang. Visual autoregressive modeling: Scalable image generation via next-scale prediction. *arXiv preprint arXiv:2404.02905*, 2024. 2, 3, 4
- [55] Aaron Van Den Oord, Oriol Vinyals, et al. Neural discrete representation learning. *Advances in neural information processing systems*, 30, 2017. 3
- [56] Peng Wang, An Yang, Rui Men, Junyang Lin, Shuai Bai, Zhikang Li, Jianxin Ma, Chang Zhou, Jingren Zhou, and Hongxia Yang. Ofa: Unifying architectures, tasks, and modalities through a simple sequence-to-sequence learning framework. In *International conference on machine learning*, pages 23318–23340. PMLR, 2022. 3
- [57] Peng Wang, Shuai Bai, Sinan Tan, Shijie Wang, Zhihao Fan, Jinze Bai, Keqin Chen, Xuejing Liu, Jialin Wang, Wenbin Ge, et al. Qwen2-vl: Enhancing vision-language model’s perception of the world at any resolution. *arXiv preprint arXiv:2409.12191*, 2024. 3
- [58] Wenhai Wang, Zhe Chen, Xiaokang Chen, Jiannan Wu, Xizhou Zhu, Gang Zeng, Ping Luo, Tong Lu, Jie Zhou, Yu Qiao, et al. Visionllm: Large language model is also an open-ended decoder for vision-centric tasks. *Advances in Neural Information Processing Systems*, 36:61501–61513, 2023. 1
- [59] Weihang Wang, Qingsong Lv, Wenmeng Yu, Wenyi Hong, Ji Qi, Yan Wang, Junhui Ji, Zhuoyi Yang, Lei Zhao, Song XiXuan, et al. Cogvlm: Visual expert for pretrained language models. *Advances in Neural Information Processing Systems*, 37:121475–121499, 2025. 5
- [60] Cong Wei, Haoxian Tan, Yujie Zhong, Yujie Yang, and Lin Ma. Lasagna: Language-based segmentation assistant for complex queries. *arXiv preprint arXiv:2404.08506*, 2024. 3, 6, 7
- [61] Jiannan Wu, Muyan Zhong, Sen Xing, Zeqiang Lai, Zhaoyang Liu, Zhe Chen, Wenhai Wang, Xizhou Zhu, Lewei Lu, Tong Lu, et al. Visionllm v2: An end-to-end generalist multimodal large language model for hundreds of vision-language tasks. *Advances in Neural Information Processing Systems*, 37:69925–69975, 2025. 2, 6, 7
- [62] Zhiyu Wu, Xiaokang Chen, Zizheng Pan, Xingchao Liu, Wen Liu, Damai Dai, Huazuo Gao, Yiyang Ma, Chengyue Wu, Bingxuan Wang, et al. Deepseek-vl2: Mixture-of-experts vision-language models for advanced multimodal understanding. *arXiv preprint arXiv:2412.10302*, 2024. 1, 3
- [63] Zhuofan Xia, Dongchen Han, Yizeng Han, Xuran Pan, Shiji Song, and Gao Huang. Gsva: Generalized segmentation via multimodal large language models. In *Proceedings of the IEEE/CVF Conference on Computer Vision and Pattern Recognition*, pages 3858–3869, 2024. 3, 6, 7
- [64] Jinjin Xu, Liwu Xu, Yuzhe Yang, Xiang Li, Fanyi Wang, Yanchun Xie, Yi-Jie Huang, and Yaqian Li. u-llava: Unifying multi-modal tasks via large language model. *arXiv preprint arXiv:2311.05348*, 2023. 2, 6, 7
- [65] Cilin Yan, Haochen Wang, Shilin Yan, Xiaolong Jiang, Yao Hu, Guoliang Kang, Weidi Xie, and Efstratios Gavves. Visa: Reasoning video object segmentation via large language models. In *European Conference on Computer Vision*, pages 98–115. Springer, 2024. 7
- [66] Charig Yang, Weidi Xie, and Andrew Zisserman. It’s about time: analog clock reading in the wild. In *Proceedings of the IEEE/CVF Conference on Computer Vision and Pattern Recognition*, pages 2508–2517, 2022. 5
- [67] Senqiao Yang, Tianyuan Qu, Xin Lai, Zhuotao Tian, Bohao Peng, Shu Liu, and Jiaya Jia. An improved baseline for reasoning segmentation with large language model. *CoRR*, 2023. 3, 5
- [68] Zhengyuan Yang, Zhe Gan, Jianfeng Wang, Xiaowei Hu, Faisal Ahmed, Zicheng Liu, Yumao Lu, and Lijuan Wang. Unitab: Unifying text and box outputs for grounded vision-language modeling. In *European Conference on Computer Vision*, pages 521–539. Springer, 2022. 3
- [69] Yuan Yao, Tianyu Yu, Ao Zhang, Chongyi Wang, Junbo Cui, Hongji Zhu, Tianchi Cai, Haoyu Li, Weilin Zhao, Zhihui He, et al. Minicpm-v: A gpt-4v level mllm on your phone. *arXiv preprint arXiv:2408.01800*, 2024. 1, 3
- [70] Haoxuan You, Haotian Zhang, Zhe Gan, Xianzhi Du, Bowen Zhang, Zirui Wang, Liangliang Cao, Shih-Fu Chang, and Yinfei Yang. Ferret: Refer and ground anything anywhere at any granularity. *arXiv preprint arXiv:2310.07704*, 2023. 3
- [71] Jiahui Yu, Yuanzhong Xu, Jing Yu Koh, Thang Luong, Gunjan Baid, Zirui Wang, Vijay Vasudevan, Alexander Ku, Yinfei Yang, Burcu Karagol Ayan, et al. Scaling autoregressive models for content-rich text-to-image generation. *arXiv preprint arXiv:2206.10789*, 2(3):5, 2022. 3

- [72] Licheng Yu, Patrick Poirson, Shan Yang, Alexander C Berg, and Tamara L Berg. Modeling context in referring expressions. In *Computer Vision—ECCV 2016: 14th European Conference, Amsterdam, The Netherlands, October 11–14, 2016, Proceedings, Part II 14*, pages 69–85. Springer, 2016. [5](#), [2](#)
- [73] Longhui Yu, Weisen Jiang, Han Shi, Jincheng Yu, Zhengying Liu, Yu Zhang, James T Kwok, Zhenguo Li, Adrian Weller, and Weiyang Liu. Metamath: Bootstrap your own mathematical questions for large language models. *arXiv preprint arXiv:2309.12284*, 2023. [5](#)
- [74] Qihang Yu, Mark Weber, Xueqing Deng, Xiaohui Shen, Daniel Cremers, and Liang-Chieh Chen. An image is worth 32 tokens for reconstruction and generation. *arXiv preprint arXiv:2406.07550*, 2024. [2](#), [3](#), [5](#)
- [75] Xiang Yue, Xingwei Qu, Ge Zhang, Yao Fu, Wenhao Huang, Huan Sun, Yu Su, and Wenhui Chen. Mammoth: Building math generalist models through hybrid instruction tuning. *arXiv preprint arXiv:2309.05653*, 2023. [5](#)
- [76] Tao Zhang, Xiangtai Li, Hao Fei, Haobo Yuan, Shengqiong Wu, Shunping Ji, Chen Change Loy, and Shuicheng Yan. Omg-llava: Bridging image-level, object-level, pixel-level reasoning and understanding. *arXiv preprint arXiv:2406.19389*, 2024. [1](#), [2](#), [3](#), [6](#)
- [77] Yichi Zhang, Ziqiao Ma, Xiaofeng Gao, Suhaila Shakiah, Qiaozi Gao, and Joyce Chai. Groundhog: Grounding large language models to holistic segmentation. In *Proceedings of the IEEE/CVF conference on computer vision and pattern recognition*, pages 14227–14238, 2024. [6](#), [7](#)
- [78] Zheng Zhang, Yeyao Ma, Enming Zhang, and Xiang Bai. Psalm: Pixelwise segmentation with large multi-modal model. In *European Conference on Computer Vision*, pages 74–91. Springer, 2024. [1](#), [2](#), [3](#), [6](#), [7](#), [4](#)
- [79] Bo Zhao, Boya Wu, Muiyang He, and Tiejun Huang. Svit: Scaling up visual instruction tuning. *arXiv preprint arXiv:2307.04087*, 2023. [5](#)
- [80] Tianyu Zheng, Ge Zhang, Tianhao Shen, Xueling Liu, Bill Yuchen Lin, Jie Fu, Wenhui Chen, and Xiang Yue. Open-codeinterpreter: Integrating code generation with execution and refinement. *arXiv preprint arXiv:2402.14658*, 2024. [5](#)
- [81] Bolei Zhou, Hang Zhao, Xavier Puig, Sanja Fidler, Adela Barriuso, and Antonio Torralba. Scene parsing through ade20k dataset. In *Proceedings of the IEEE conference on computer vision and pattern recognition*, pages 633–641, 2017. [5](#)
- [82] Bolei Zhou, Hang Zhao, Xavier Puig, Tete Xiao, Sanja Fidler, Adela Barriuso, and Antonio Torralba. Semantic understanding of scenes through the ade20k dataset. *International Journal of Computer Vision*, 127:302–321, 2019. [6](#)
- [83] Chaoyang Zhu, Yiyi Zhou, Yunhang Shen, Gen Luo, Xingjia Pan, Mingbao Lin, Chao Chen, Liujuan Cao, Xiaoshuai Sun, and Rongrong Ji. Seqtr: A simple yet universal network for visual grounding. In *European Conference on Computer Vision*, pages 598–615. Springer, 2022. [1](#), [3](#)
- [84] Lanyun Zhu, Tianrun Chen, Deyi Ji, Jieping Ye, and Jun Liu. Llafs: When large language models meet few-shot segmentation. In *Proceedings of the IEEE/CVF Conference on Computer Vision and Pattern Recognition*, pages 3065–3075, 2024. [1](#), [2](#), [3](#)
- [85] Yongxin Zhu, Bocheng Li, Yifei Xin, and Linli Xu. Addressing representation collapse in vector quantized models with one linear layer. *arXiv preprint arXiv:2411.02038*, 2024. [3](#)
- [86] Xueyan Zou, Jianwei Yang, Hao Zhang, Feng Li, Linjie Li, Jianfeng Wang, Lijuan Wang, Jianfeng Gao, and Yong Jae Lee. Segment everything everywhere all at once. *Advances in neural information processing systems*, 36:19769–19782, 2023. [3](#)



# HiMTok: Learning Hierarchical Mask Tokens for Image Segmentation with Large Multimodal Model

## Supplementary Material

### A. Limitations

While HiMTok enables large multimodal models to acquire native (referring) image segmentation capabilities in a concise and natural manner, the current work has some limitations. (1) The length of predicted mask tokens is predefined. LMMs are not able to determine it adaptively according to object shape complexities. (2) The current model is relatively passive for object segmentation, due to the use of passive segmentation training data. We need to specify referring expressions to clarify the expected objects, rather than let the model itself segment all objects of interest at once. (3) It appears challenging for fine-grained region segmentation in the current version (See Appendix F). The lack of multi-scale feature design may cause the loss of fine-grained features.

### B. Multi-grained mask labels

The multi-grained mask labels are important in the hierarchical mask loss. We have tried to use only the final mask label to supervise each granularity level, but the loss is relatively high due to the insufficient representation by few mask tokens. This also causes unstable training and even side influence on the general capability of LMM. In experiments, we find that few mask tokens are usually de-tokenized into Gaussian distribution maps, which inspire us to make multi-grained mask labels by Gaussian blurring.

Under the setting of mask token length to 32, we first choose a full-level (*i.e.*, 32 tokens) sequence and 3 random levels that are sampled by  $p_l = \frac{1}{l+8}, 1 \leq l < 32$ . For each partial level  $l$ , we produce a kernel following the 2D Gaussian distribution function  $\mathcal{N}(\mu, \sigma)$ , where  $\mu = 0$ , and  $\sigma = \frac{100}{l+1} - 2$ . Then the kernel is applied to the full-level mask image to obtain the mask label at level  $l$ . Fig. 8 visualizes some examples with different granularity levels.

### C. Finetuning SAM

Despite the fact that LMM equipped with HiMTok, without relying on segmentation foundation models, has achieved state-of-the-art performance on various segmentation tasks, further improvements can still be expected by feeding the mask from our de-tokenizer into SAM [26]. This post-refinement module can be defined as a mapping  $\mathcal{R} : (\mathcal{I}, \mathcal{M}_{in}) \rightarrow \mathcal{M}_{out}$ , where  $\mathcal{M}_{in}$  is the output mask by our HiMTok-equipped LMM, and  $\mathcal{I}$  is the input image. However, we find that the native SAM given  $\mathcal{M}_{in}$  tends to segment fine-grained parts of objects or generate mask maps



Figure 7. Further improvements by finetuned SAM.

with holes, even when the given mask clearly covers large and unambiguous regions, as visualized in Fig. 7.

To adapt to our case, we finetune the mask decoder and the mask convolution layers in SAM. The input mask  $\mathcal{M}_{in}$  is augmented in two aspects. On the one hand, the number of mask tokens passed to the de-tokenizer is randomly reduced so that the fine-grained shape details may be lost. On the other hand, the de-tokenized mask is processed by random morphological augmentation, including dilation and erosion. As a result, the finetuned SAM is able to refine imperfect masks. Qualitative results are shown in Fig. 7. The finetuned SAM improve the edge details of the segmentation masks.

### D. More details on training

In stage-3, some datasets are down-sampled. Details are listed in Tab. 9. The initial learning rate is  $4e - 5$  in stage 2,  $2e - 5$  in stage 3, and  $8e - 6$  in task finetuning. The GPU hours (Nvidia A800) for our 3 stages are: 192, 1920 and 640.

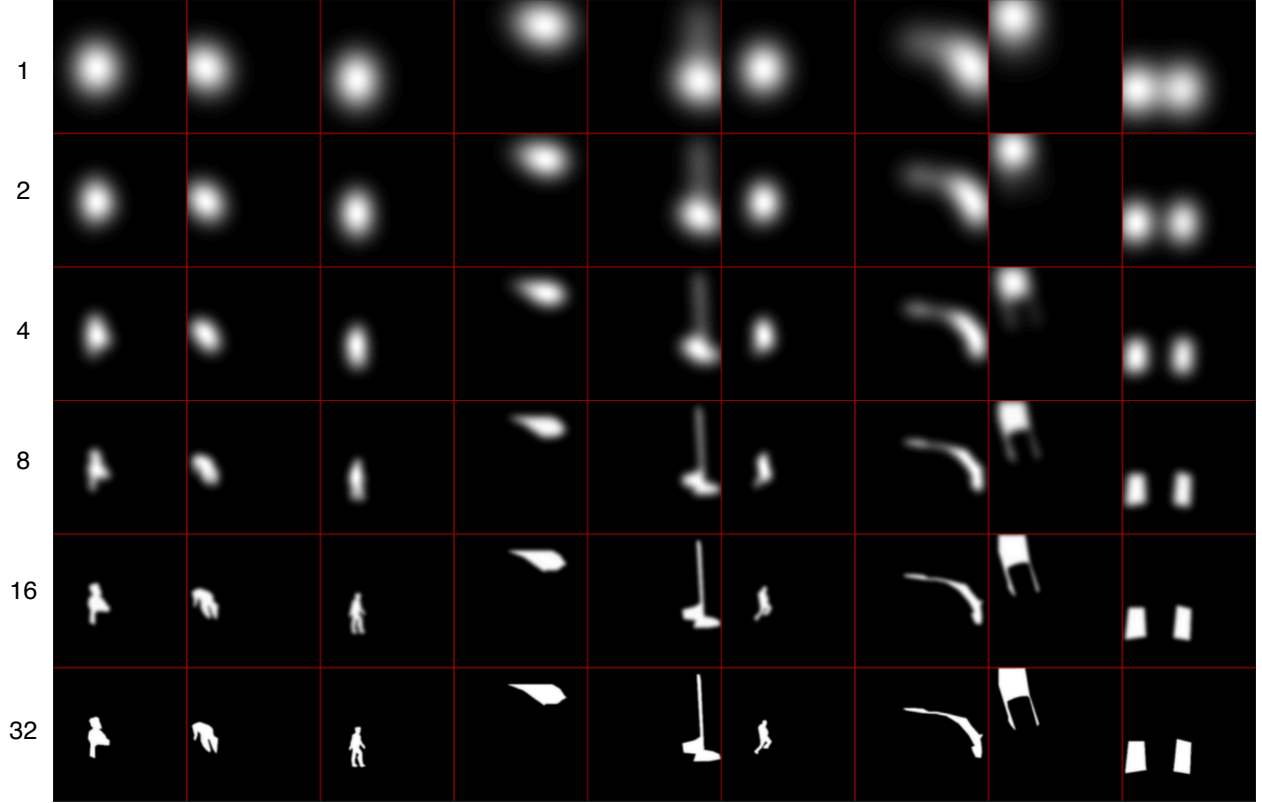


Figure 8. The Gaussian-blurred mask label at different levels.

Table 9. The amount of samples in down-sampled datasets for stage-3.

Dataset	stage-2	stage-3
SA1B	1M	250K
COCO-Rem	350K	35K
COCO-Stuff	500K	50K
COCO-Panoptic	233K	116K
PartImageNet	20K	4K
Objects365	450K	90K

## E. Mask Perception

One key feature of our method is the consistence of mask representation in LLM input and output. The image segmentation tasks are all text-to-mask. As a supplement, we devise a mask-to-text task, Mask Perception<sup>†</sup>, which aims for fine-grained understanding. Mask Perception (MaP) mirrors RES: models are required to choose a matched expression, given an image, an object mask and several expression options.

<sup>†</sup>[https://huggingface.co/datasets/yayafengzi/Mask\\_Perception](https://huggingface.co/datasets/yayafengzi/Mask_Perception)

The training and test sets are built based on Ref-COCO+/g [40, 72]. We randomly sample some examples and reverse the positions of masks and expressions in multiple-choice questions. One or more positive options are possible in the training set, while only one positive option is available in the test set to simplify evaluation. Negative expression options are selected from other objects in the same image or from different images. This approach encourages the model to distinguish the distinctive features of various parts. Statistics are shown in Tab. 10.

We have tried to compare our method with PSALM [78] which performs interactive segmentation well. However, we found that PSALM does not follow instructions well in our MaP test set. Therefore, we compared our method both with and without the MaP training set. As shown in Tab. 11, our method inherently has a good perception of input masks. With the addition of the MaP training set, the mask perception capability is significantly improved.

## F. Results on fine-grained regions

Given that HiMTok decodes masks directly via mask tokens, a natural concern is whether it can maintain high seg-

Table 10. Statistics of Mask Perception. The data source is RefCOCO+/g.

data split	source	single/multiple choices	No.
Training	train	multiple	190k
Test	val & test	single	10k

Table 11. Accuracy on mask perception.

w/ MaP	×	✓
Acc	63.1	81.8

mentation quality for fine-grained regions without leveraging the fine-grained features of the original image.

Here we show the results on small object segmentation in RefCOCO+/g. Objects whose mask areas occupy less than 4% of the image are considered as small, resulting in 12.8% samples. Shown in Tab. 12, the cIoUs of ours still have significant priority compared to PSALM [78]. However, the cIoU scores fall significantly behind the overall performance (Tab. 2), which highlights a common challenge.

We also review the segmentation boundaries. Bfscore (a boundary-aware F1 metric) on RefCOCO (val) is reported: our method gets 0.927, which is competitive to PSALM (0.936). PSALM integrates Mask2Former that is favored by multi-scale features. We believe there are rooms for future exploration in our paradigm.

## G. Results on general image understanding

Here, we list additional results on general image understanding. Our model is not finetuned on these tasks.

We compare methods on MME [19] Perception, VQAv2 [20], and POPE [32]. As shown in Tab. 13, our method is comparable to state-of-the-art LMMs, except in the areas of landmarks, artwork, and OCR, where we do not specially utilize corresponding training data in this work. We can conclude that LMM<sub>HiMTok</sub> is a comprehensional and general LMM.

## H. More visualizations

Fig. 9 shows more interesting and challenging cases. Fig. 10 illustrates how we implement referring image segmentation in conversations. This is what we do when evaluating our model on gRefCOCO, ReasonSeg, and open-vocabulary segmentation.

## I. Prompt design

We prepared plentiful prompt templates for instruction tuning on segmentation and visual grounding.

For the bidirectional information flow between segmentation and grounding, Tabs. 14 and 15 list templates for

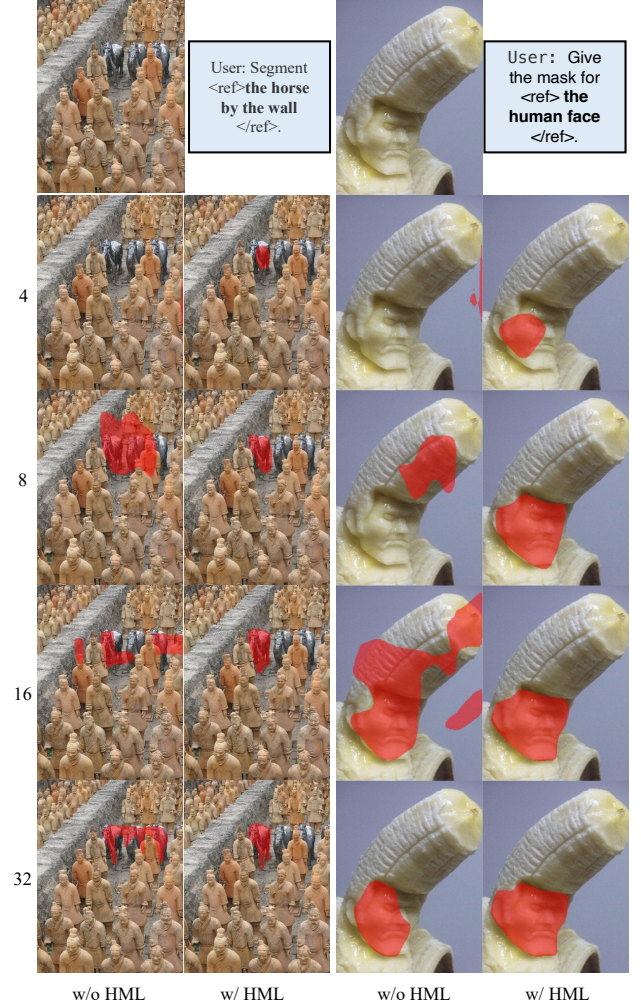


Figure 9. More examples on the coarse-to-fine mask token representation with and without HML.

mask-to-box, and Tabs. 16 and 17 are for coordinate-to-mask. Tab. 18 list templates for segmentation-only responses. Templates in Tab. 19 are used to specify the mask token length from LMM. If visual grounding is the only target without mask tokens, we can refer to Tab. 20.



Table 12. Results on small object segmentation.

	Ref COCO			Ref COCO+			Ref COCOg	
	val	testA	testB	val	testA	testB	val	test
PSALM [78]	64.50	68.43	57.31	45.58	55.89	38.14	51.10	48.78
ours	67.15	75.00	60.34	56.81	63.06	48.29	57.71	55.99

Table 13. Results on general image understanding.

Method	MME										VQAv2	POPE
	existence	count	position	color	posters	celebrity	scene	landmark	artwork	OCR		
PSALM [78]	-	-	-	-	-	-	-	-	-	-	62.3	80.3
InternVL2.5-8B [11]	<b>200</b>	<b>170</b>	163	<b>180</b>	<b>169</b>	<b>140</b>	155	<b>172</b>	<b>160</b>	<b>178</b>	-	<b>90.6</b>
LMM <sub>HiMTok</sub> -8B	<b>200</b>	160	<b>166</b>	<b>180</b>	164	132	<b>163</b>	132	120	88	<b>75.9</b>	86.8

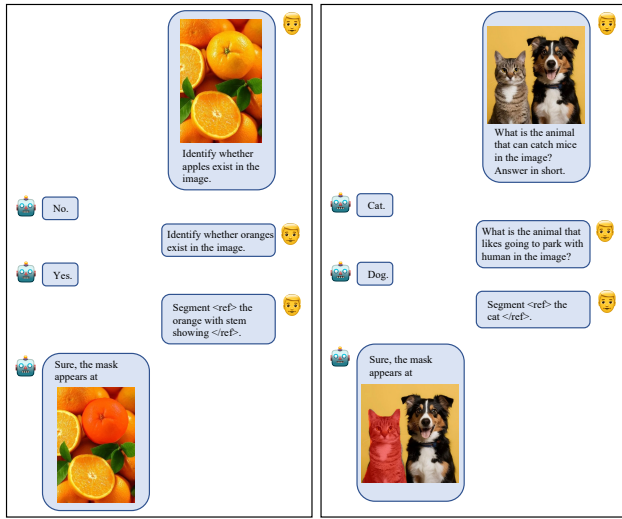


Figure 10. Referring image segmentation in conversation.

Table 14. Templates of instruction for segmentation then grounding.

- "First create the segmentation mask for <ref>{</ref>, then identify its bounding box."
- "Begin by generating the mask for <ref>{</ref>, followed by determining its box coordinates."
- "Start with the detailed mask of <ref>{</ref>, then locate its containing box."
- "Initially segment <ref>{</ref>, then find its bounding box region."
- "First produce the mask for <ref>{</ref>, then specify its box location."
- "Commence with the mask of <ref>{</ref>, then determine its box boundaries."
- "Start by segmenting <ref>{</ref>, then outline its bounding region."
- "First extract the mask of <ref>{</ref>, then mark its box coordinates."
- "Begin with the precise mask for <ref>{</ref>, then identify its box location."
- "Initially create the mask for <ref>{</ref>, then define its bounding box."

Table 15. Templates of response for segmentation then grounding.

- "Certainly, you can find the mask at {</ref>, and the box is represented as <box>{</box>."
- "Of course, the mask located is {</ref>, while the box is shown as <box>{</box>."
- "Absolutely, the mask is situated at {</ref>, with the box described as <box>{</box>."
- "Sure, the mask appears at {</ref>, and here's the box: <box>{</box>."
- "Indeed, the mask can be found at {</ref>, with the box marked as <box>{</box>."
- "OK, the mask is at {</ref>, and the box is indicated as <box>{</box>."
- "Affirmative, you have the mask at {</ref>, and the box is designated <box>{</box>."
- "Got it, the mask is at {</ref>, and you will see the box like <box>{</box>."
- "Sure, the mask appears at {</ref>, and here is the box represented: <box>{</box>."
- "Yes indeed, find the mask at {</ref>, and the box outlined as <box>{</box>."

Table 16. Templates of instruction for box/point-prompted segmentation in SAIB.

- "Generate the segmentation mask for the object located within the bounding box <box>{</box> and at the points {</ref> in the provided image."
- "Extract the mask for the object inside the <box>{</box> bounding box and corresponding to the points {</ref> in the given image."
- "Create the mask for the object found in the region defined by <box>{</box> and identified by the points {</ref> in this image."
- "Identify the object mask within the bounding box <box>{</box> and marked by the points {</ref> in the image."
- "Acquire the segmentation mask of the object enclosed by <box>{</box> and situated at the points {</ref> in the image."
- "Determine the mask for the object that is located within the area specified by <box>{</box> and identified by the points {</ref> in the image."
- "Produce the mask for the object situated in the <box>{</box> box and at the points {</ref> within the image."
- "Locate the mask for the object that lies inside the <box>{</box> boundaries and corresponds to the points {</ref> in the image."
- "Segment the mask for the object found within the bounds of <box>{</box> and marked at the points {</ref> in the given image."
- "Outline the mask of the object residing within the box <box>{</box> and corresponding to the points {</ref> in the image."



Table 17. Templates of instruction for point-prompted segmentation in SAIB.

- “Generate the segmentation mask for the object located at the points {} in the provided image.”
- “Extract the mask for the object that corresponds to the points {} in the given image.”
- “Create the mask for the object identified by the points {} in this image.”
- “Identify the object mask corresponding to the points {} in the image.”
- “Acquire the segmentation mask of the object marked at the points {} in the image.”
- “Determine the mask for the object located at the specified points {} in the image.”
- “Produce the mask for the object situated at the points {} within the image.”
- “Locate the mask for the object that is identified by the points {} in the image.”
- “Segment the mask for the object found at the points {} in the given image.”
- “Outline the mask of the object located at the specified points {} in the image.”

Table 18. Templates of response for segmentation only.

- “Certainly, the mask is located at {}.”
- “Of course, you can find the mask at {}.”
- “Absolutely, the mask is available at {}.”
- “Sure, the mask is positioned at {}.”
- “Indeed, the mask appears at {}.”
- “OK, the mask is situated at {}.”
- “Affirmative, the mask can be found at {}.”
- “Got it, the mask is at {}.”
- “Sure, the mask is present at {}.”
- “Yes indeed, you will find the mask at {}.”

Table 19. Templates of instruction for segmentation with specified token lengths.

- “First create the segmentation mask for <ref>{}</ref>{} by {} tokens, then identify its bounding box.”
- “Begin by generating the mask for <ref>{}</ref>{} by {} tokens, followed by determining its box coordinates.”
- “Start with the detailed mask of <ref>{}</ref>{} by {} tokens, then locate its containing box.”
- “Initially segment <ref>{}</ref>{} by {} tokens, then find its bounding box region.”
- “First produce the mask for <ref>{}</ref>{} by {} tokens, then specify its box location.”
- “Commence with the mask of <ref>{}</ref>{} by {} tokens, then determine its box boundaries.”
- “Start by segmenting <ref>{}</ref>{} by {} tokens, then outline its bounding region.”
- “First extract the mask of <ref>{}</ref>{} by {} tokens, then mark its box coordinates.”
- “Begin with the precise mask for <ref>{}</ref>{} by {} tokens, then identify its box location.”
- “Initially create the mask for <ref>{}</ref>{} by {} tokens, then define its bounding box.”

Table 20. Templates of for visual grounding without mask tokens.

- Instructions**
- “Please provide the bounding box of <ref>{}</ref>.”
  - “Locate the bounding box for <ref>{}</ref>.”
  - “Identify the box coordinates of <ref>{}</ref>.”
  - “Determine the bounding region for <ref>{}</ref>.”
  - “Find the box boundaries of <ref>{}</ref>.”
  - “Mark the box location of <ref>{}</ref>.”
  - “Specify the box coordinates for <ref>{}</ref>.”
  - “Outline the bounding box of <ref>{}</ref>.”
  - “Can you show the box for <ref>{}</ref>?”
- Responses**
- “Certainly, the box is located at <box>{}</box>.”
  - “Of course, here’s the bounding box: <box>{}</box>.”
  - “The requested box coordinates are <box>{}</box>.”
  - “Found the bounding region: <box>{}</box>.”
  - “Here’s the box location: <box>{}</box>.”
  - “The object’s box is marked as <box>{}</box>.”
  - “Bounding box determined: <box>{}</box>.”
  - “Located the boundaries at <box>{}</box>.”